Open Access

SCHOLARENA

Journal of Environmental Pollution and Management

RESEARCH ARTICLE

ISSN: 2639-7269

The Applicability of Fe (III)-Chitosan Complex for the Sorption of Single-Phase Acid Blue-15 Dye from Water

Al-Anber MA* and Al-Qaisi W

Department of Chemistry, Faculty of Sciences, Mu´tah University, Al-Karak, Jordan

***Corresponding author:** Al-Anber MA, Department of Chemistry, Faculty of Sciences, Mu´tah University, P.O. Box 7, 61710 Al-Karak, Jordan, Tel: +966-(0)79-2301035; E-mail: masachem@mutah.edu.jo

Citation: Al-Anber MA, Al-Qaisi W (2019) The Applicability of Fe (III)-Chitosan Complex for the Sorption of Single-Phase Acid Blue-15 Dye From Water. J Environ Pollut Manage 2: 105

Abstract

The objective of this work concern with the applicability of Fe (III)-chitosan complex for the adsorption of single-phase Acid Blue-15 (AB-15) dye from water through a batch process. The maximum removal of dye increased with the increase of pH, the dosage of Chitosan-Fe (III) adsorbent and temperature of the reaction vessel. However, the percentage of removal decreases with the increase in the initial concentration of the AB-15 solution. The results show that the pH of the interaction medium shows a significant influence in the adsorption process achieving the maximum removal in the basic medium. The adsorption of AB-15 on the Fe (III)-chitosan complex sorbent fits better with the Langmuir (R^2 = 0.998) than the Freundlich model. The adsorption Kinetics follows the pseudo-second-order (R^2 > 0.998) and not the pseudo-first-order model. The obtained results of this study show that Fe (III)-chitosan complex sorbent has a potential application as a membrane to remove the AB-15 from industrial effluents.

Keywords: Acid Blue-15; Dye; Sorption; Fe (III)-chitosan complex; Langmuir; Pseudo-second order

Introduction

It is known that dyes contaminate the water medium through industrial processes and washing clothes and textiles [1-2]. Acid Blue-15 dye is considered as one of these dyes that has health and environmental impacts [3-5]. Acid Blue-15 dye is a type of as azo dyes, which has a complex and resonance-stabilized triphenylmethane (TPM). This complex resists degradation in the environment causing a threat for human life. Therefore, our efforts are going toward the removal of such dyes from the aqueous system. The traditional processes focus on the removal of dyes by using physical and chemical methods such as coagulation [6], membrane filtration [7], photocatalytic degradation [8-9], Nano filtration and ozonolysis, oxidation [10], and microbiological decomposition [11]. In general, these processes break down the azo dyes to form carcinogenic aryl-amines; it decomposes to simple metabolic intermediates. This process leads to a more and more increasing problem. Wherein, the decomposition procedures are not efficient because many dyes cannot be easily decomposed [12]. Therefore, the most efficient one is the adsorption process [13-16]. Several cheap and safe adsorbent is used and investigated for removing dyes from water, such as: orange peel [17], dolomitic [18], calcine alunite [19], clay [20], bottom ash [21], zeolite [22], Chitosan [23], Bentonite [24], silica fume [25], *Azolla filiculoides* [26], rice husk [27], canola [28] and Lemna minor [29]. More example for a removal of AB15 dye from aqueous solutions are Red mud [30], wood and sawdust [31], fly ash [32], wheat straw [33], apple pomace [33], orange peel [34-36], banana peel [37], leaf [38], Soybean cake [39], eggshell membrane [40], lignocellulosic waste biomass activated carbon [41]. Therefore, in literature, we find little works in the removal and sorption of Acid Blue 15. These articles focus into the utilization of the various adsorbents, for example, *macroalga Azolla filiculoides* [42], Activated carbons of sunflower seed hull [43,44], *Azolla rongpong* [45], *Azolla filiculoides* biomass [46], immobilized cell bioreactor [47], activated carbon of melon seed hull [48], Activated carbon of Delonix regia (DR) seed pod [49], Bagasse, groundnut shells, cow dung, pea shells, wheat straw, and tea leaves [50], β-Cyclodextrin (CD), hydroxypropyl β-cyclodextrin (HPCD), poly (vinyl alcohol) (PVOH) [51], activated carbon from pomelo skin [52], and freshwater algae [53].

Recently, our research group utilizes the chitosan as flocculating and chelating agents in wastewater treatment and drinking water for removing heavy metals and synthetic dyes as a potential application as membrane filters. One of our recent publication concerns with the sorption of Acid Blue-15 (AB-15) dye from the water by using chitosan. The batch process achieves the highest removal percentage (99%) during the first 50 minutes (equilibrium time) of batch physisorption [54]. The new reported study, concerning with the sorption of iron (III) ion from water by chitosan [55], guide us to produce Fe (III)-chitosan complex as an adsorbent for

removal of anionic dyes such as AB-15. This may produce large macromolecular cross linked chitosan; however it increase the positive.

Up to date, we do not find any work related to the sorption of the Acid Blue-15 by using Fe (III)-chitosan complex sorbent. Therefore, the main purpose of the study is to utilize the Fe (III)-chitosan complex as adsorbent to remove of Acid Blue dye from water. The objectives of this work is: **(i)** to determine maximum removal of AB-15 by using different environmental parameters of interaction, such as initial concentration of AB-15, dosage of adsorbent, contact time and pH, **(ii)** to study the thermodynamic and kinetic model parameters, and **(iii)** to estimate the interaction mechanism between AB-15 and Fe (III)-chitosan complex sorbent.

Material and Methods

Preparation of Fe (III)-chitosan complex sorbent

Chitosan (Synonym: Deacetylated chitin, Poly (D-glucosamine) is used as received from Sigma-Aldrich without further purification as medium molecular weight. The mass median diameters of the Chitosan flakes were estimated to be (228 ± 5)μm. Iron (III)-chitosan complex formed by adsorption of iron(III) ion onto chitosan as either Penta- or hexacoordinated Fe (III) [55]. Twenty milligrams of the chitosan sample {in flakes forms (228 ± 5) μm}, and a 4-mL sample of an aqueous iron (III) ($Fe(NO_3)_3.9H_2O$ solution with a 100 mg L^{-1} concentration at pH = 1.42 of 1% HNO_3 were mixed in the reaction vessel and thermostatically maintained at 80 rpm and 30 °C for 40 minutes.

Reagents

All chemicals were used as received as an analytical grade. Acid Blue-15 (AB-15) was purchased from Alvan Sabet CO (M_{wt} = 775.95 g/mol; the chemical formula is $C_{42}H_{46}N_3NaO_6S_2$). The stock solution (1000 mg L^{-1}) was prepared by dissolving a stoichiometric amount of AB-15 powders in 1 L of distilled water. Standard solutions of AB-15 (10, 30, 50, 70, and 100 mg L^{-1}) were prepared by appropriate dilution from 1000 mg L^{-1} stock solution. An "initial" pH and its subsequent adjustment for all experimental runs were conducted less than 7.00 at the maximum value. NaOH (0.1 mol L^{-1}), HCl (0.1 mol L^{-1}) and HNO_3 (65%) were purchased from Merck (Darmstadt, Germany). Chitosan (Synonym: Deacetylated chitin, Poly (D-glucosamine) is used as received from Sigma-Aldrich without further purification as medium molecular weight. The mass median diameters of the Chitosan flakes were estimated to be (228 ± 5) μm. The salt of Iron (III) ion $Fe(NO_3)_3.9H_2O$ was purchased by commercial providers from Fluka Chemika.

Apparatus and instruments

AB-15 absorbs light in the field between about 530 to 700 nm so that the peak is at about 560 nm. Therefore, the AB-15 concentration in the solution was measured by using the Ultraviolet Visible Spectroscopy (Shimadzu UV-1800 UV-Vis Spectrophotometer). All the reported results were the average of at least triplicate measurements at 560 nm. The mixtures were mixed by a thermostatic mechanical shaker at constant temperature (25, 35, 45 and 55 °C, Isothermal Gefellschaft Fur 978). To ensure accuracy in the preparation, analytical balance is used (Sartorius, CP324-S/ management system certified according to ISO 9001). The chemical functional groups of the Fe (III)-Chitosan complex are detected by Fourier-Transform Infrared Spectroscopy (Thermo Scientific Nicolet IR200 FT-IR, 400-4000 cm^{-1}).

Equilibrium studies

The batch removal of the AB-15 was calculated from the mass balance, which was stated as the amount of AB-15 adsorbed onto the solid particles of the Fe (III)-chitosan complex sorbent. It equals a number of AB-15 removed from the aqueous solution. Mathematically can be expressed in equations 1-2 [54,56,57]:

$$q_e = \frac{(C_i - C_e)}{S} \quad (1)$$

$$q_t = \frac{(C_i - C_t)}{S} \quad (2)$$

Where

q_e: AB-15 amount adsorbed on the Fe (III)-chitosan sorbent surface at equilibrium (mg g^{-1}).

q_t: AB-15 amount adsorbed on Fe (III)-chitosan sorbent surface at a specific time (mg g^{-1}).

C_i: Initial concentration of AB-15 in the aqueous solution (mg L^{-1}).

C_e: Equilibrium concentration or final concentration of AB-15 in the aqueous solution (mg L^{-1}).

C_t: The final concentration of AB-15 in the aqueous solution (mg L^{-1}) at a specific time.

S: Dosage (slurry) concentration of Fe (III)-chitosan complex sorbent and it is expressed by:

$$S = \frac{m}{v} \quad (3)$$

Where *v* is the initial volume, of AB-15, the solution used (L) and m is the mass of Fe (III)-chitosan complex sorbent.
The percent adsorption (%) was also calculated using the following equation

$$\% \text{ adsorption} = \frac{C_i - C_e}{C_i} \times 100\% \qquad (4)$$

Effect of AB-15 Initial Concentration

Adsorption measurements were made by a batch technique at a temperature of 35 (± 1 °C). The stopper plastic flasks containing 50 mL of different initial concentrations (Ci = 10, 30, 50, 70 and 100 mg L^{-1}) of AB-15 and 2 g L^{-1} of Fe (III)-Chitosan complex were shaken vigorously using a thermostatic mechanical shaker for 50 minutes. The agitation speed (80 rpm) was kept constant for each run to ensure equal mixing. At the end of the equilibrium time, the flasks were removed from the shaker and then the supernatant solution in each flask was filtered using filter paper (Whatman No. 41). The filtrate samples were analyzed. All the reported results were the average of at least triplicate measurements.

Effect of Temperatures

The adsorption experiments were carried out by shaking vigorously the stopper plastic flasks containing 50 mL of 100 mg L^{-1} of AB-15 dye and 2 g L^{-1} of Fe (III)-Chitosan complex by using a thermostatic mechanical shaker at constant contact time (50 minutes) and agitation speed (80 rpm) with varying temperatures (25, 35, 45 and 55 °C). At the end of the equilibrium time, the flasks were removed from the shaker, and then Fe (III)-Chitosan complex particles was filtered using filter paper (Whatman No. 41). The filtrate supernatant solutions were analyzed. All the reported results were the average of at least triplicate measurements.

Effect of dosage

The adsorption experiments were carried out by a batch technique at a temperature of 35 °C (± 1 °C). Different doses of Fe (III)-Chitosan complex (2, 6, 10, 14 and 20 g L^{-1}) were placed in a 100 mL stopper plastic flask containing 50 mL of aqueous AB-15 (Ci = 100 mg L^{-1}). The solutions were shaken vigorously by using a thermostatic mechanical shaker for 50 minutes. The agitation speed (80 rpm) was kept constant for each run to ensure equal mixing. At the end of the equilibrium, the flasks were removed from the shaker, and then the solution was filtered using filter paper (Whatman No. 41). The filtrate supernatant solutions were analyzed. All the reported results were the average of at least triplicate measurements.

Effect of contact time

The sorption experiments were carried out by shaking 0.1 g of the Fe (III)-chitosan complex sorbent with 50 mL of 100 mg L^{-1} of AB-15 solution (pH_i = 7.4, dosage = 2g L^{-1}). The solutions were shaken vigorously using thermostatic mechanical shaker at constant temperature (25, 35, 45 and 55 °C). The agitation speed was fixed at 80 rpm for a known period in the interval of 0.5 to 180 minutes with increment of 10 minutes from 10 to 60 minutes, and then 30 minutes from 60 to 180 minutes. At the end of the predetermined time, the flasks were removed from the shaker and then the supernatant solution in each flask was filtered using filter paper (Whatman No. 41). The filtrate samples were analyzed. All the reported results were the average of at least triplicate measurements.

Effect of pH

The adsorption experiments were carried out by a batch technique at a temperature of 35 °C (± 1 °C). Different doses of Fe (III)-chitosan complex sorbent (2, 4, 7and 10 g L^{-1}) were placed in a 100mL stopper plastic flask containing 50mL of aqueous AB-15 (C_i = 100 mg L^{-1}). The solutions were shaken vigorously by using a thermostatic mechanical shaker for 90 minutes. The agitation speed (80 rpm) was kept constant for each run to ensure equal mixing. At the end of the equilibrium, the flasks were removed from the shaker, and then the solution was filtered using filter paper (Whatman No. 41). The filtrate supernatant solutions were analyzed. All the reported results were the average of at least triplicate measurements.

Adsorption Isotherm Models

The isotherm experiments were conducted by using 10, 30, 50, 70 and 100 mg L^{-1} of AB-15 dye solutions. The mixtures containing 0.1 g Fe (III)-chitosan complex sorbent and 50 ml of AB-15 dye solutions were stirred under the shaking conditions of 80 rpm, 50 minutes and 35 °C. Afterward, the flasks were removed from the shaker, and then Fe (III)-chitosan solid was filtered by filter paper (Whatman No. 41). The filtrate supernatant solutions were analyzed. All the reported results were the average of at least triplicate measurements.

Adsorption Kinetic Models

For the kinetic studies, a number of samples containing 0.1 g Fe (III)-chitosan complex sorbent and 50 ml of AB-15 solutions (C_i = 100 mg L^{-1}) were placed in the 100 ml flasks. The initial pH was 7. These flasks were agitated using a temperature-controlled shaker (study at various T = 25, 35, 45 and 55 °C) at 80 rpm for 50 minutes. Afterwards, the flasks were removed from the shaker at every 10 minutes in the first 60 minutes and then 30 minutes until the end of 180 minutes. The Fe (III)-chitosan complex solid

was filtered using filter paper (Whatman No. 41). The filtrate supernatant solutions were analyzed. All the reported results were the average of at least triplicate measurements.

Results and Discussion

FTIR Spectroscopy

FTIR spectra of chitosan [53] and Fe (III)-chitosan complex show that both two spectra are identical except for the loss of the peak at 1554 cm^{-1} due to N-H bending vibrations of chitosan. This can be interpreted as the formation of a Fe (III)-chitosan complex through the involvement of N atoms on the chitosan backbone. The nonexistence of any new absorption band or shifting indicates the adsorption of Fe (III) ion onto chitosan forming a weak Fe (III)-chitosan complex. Therefore, physical and chemical properties of chitosan may be modified by using Fe (III) ion to make it a suitable to capture anionic dyes and anionic pollutant species.

The sorption of AB-15 onto the Fe (III)-chitosan complex sorbent

The sorption of AB-15 onto the solid particles of the Fe (III)-chitosan complex sorbent could be performed through the suggested chemisorption mechanism through the electrostatic interaction of AB-15 with the iron onto on the Fe (III)-chitosan sorbent surface (see Scheme 1). The sorption of AB-15 onto Fe (III)-chitosan complex sorbent achieves the suggestion of a chemisorption mechanism of Lagergren pseudo-second-order model (ca. $R^2 = 0.998$). This idea can be confirmed by the FTIR spectra of Fe (III)-chitosan complex sorbent before and after sorption of AB-15 dye. In contrast with the reported of our study [54] and others [58,59], regarding the sorption of AB-15 onto chitosan only, achieve the suggestion of a physisorptions mechanism of Lagergren pseudo-first-order model.

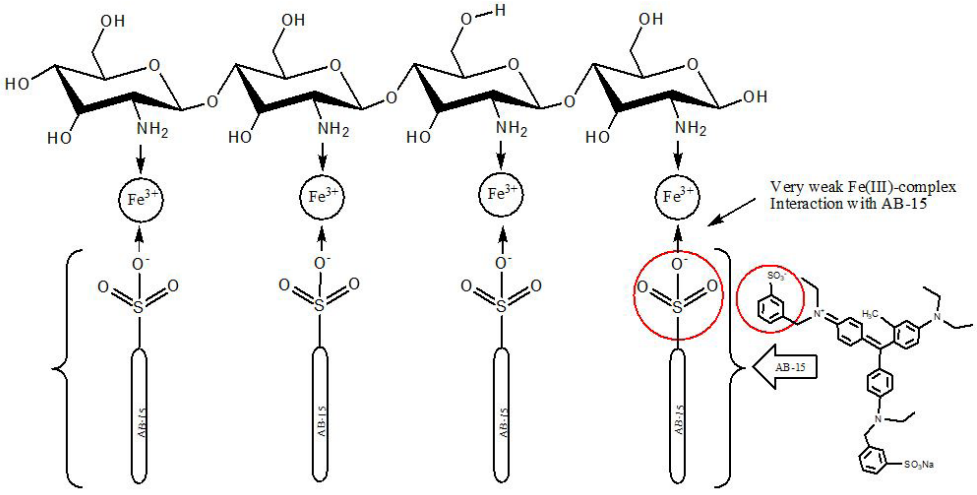

Scheme 1: The possible mechanism of adsorption of AB-15 onto Chitosan adsorbent

Effect of AB-15 Concentration

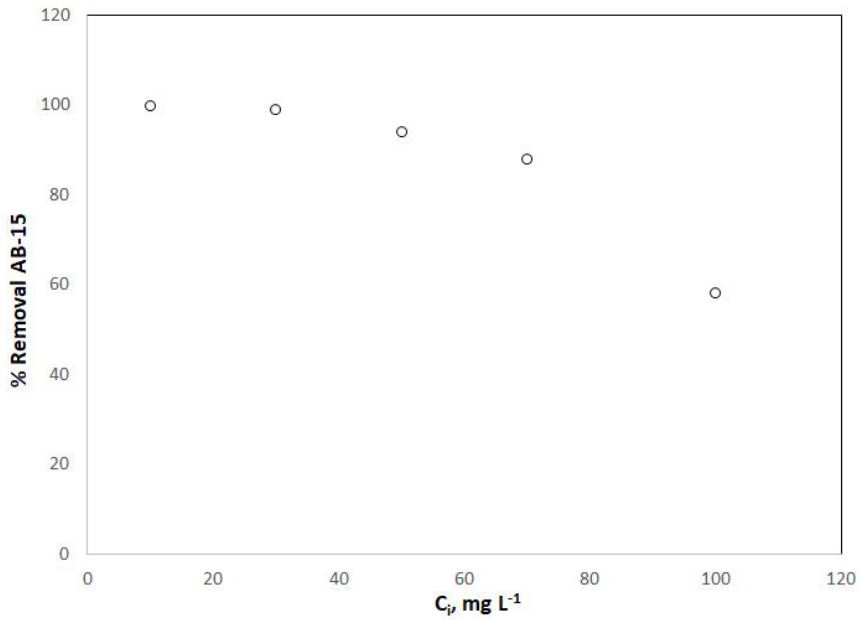

Figure 1: Effect of initial concentration of AB-15 (t = 50 min, 35 °C, 50 ml, 0.1 g Fe (III)-chitosan complex sorbent, 80 rpm)

The effect of the initial AB-15 concentration on the sorption efficiency is investigated in the concentration range of 10-100 mg L^{-1} at 35 °C. Figure 1 shows that the initial concentration of AB-15 has a highly significant influence on the sorption process; in general the percentage of removal decreases with increasing the initial concentration of AB-15 causing, which causes a decrease in the sorption efficiency of the Fe (III)-Chitosan adsorbent. This may be due to the saturation of adsorption sites on the adsorbent surface. On the other hand, the increase in initial dye concentration will cause an increase in the adsorption capacity of the adsorbent, which may be due to the high driving force for mass transfer at a high initial dye concentration. This behavior agrees relatively with the results obtained by using chitosan [54] and Red mud for removal of AB15 dye from aqueous solutions [30].

Effect of Temperature

The influence of temperature on the removal of AB-15 from the aqueous solution by using Fe (III)-chitosan complex sorbent has been studied through the applied of a variety of temperatures 25, 35, 45 and 55 °C. It is observed that the removal percentage increased with increasing temperature (Figure 2); wherein it is highly influenced by raising the value of temperatures. The maximum removal percentage at 55 °C is 85 %, while the lowest percentage is 58 % (approx.) at a temperature of 25 °C. This indicates that high temperature could enhance the chemical interaction of AB-15 with Fe (III)-chitosan sorbent surface (chemisorption) [59]. This type of interaction is not typical to the adsorption of the AB-15 dye by chitosan [54].

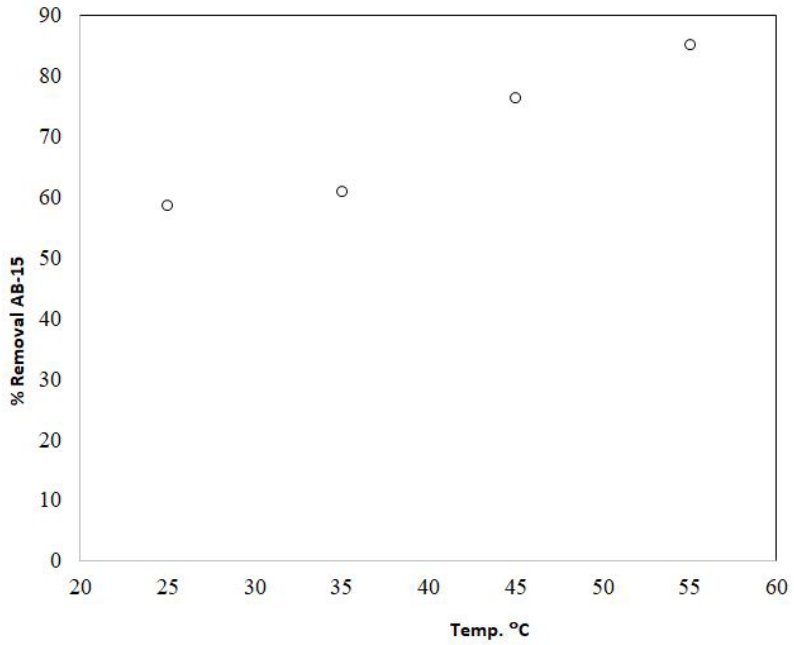

Figure 2: Effect of temperature (dosage of Fe (III)-chitosan sorbent = 2 g L^{-1}, C_i = 100 mg L^{-1}, 80 rpm, pH_i = 7.00)

Dosage effects of Fe (III)-chitosan complex sorbent

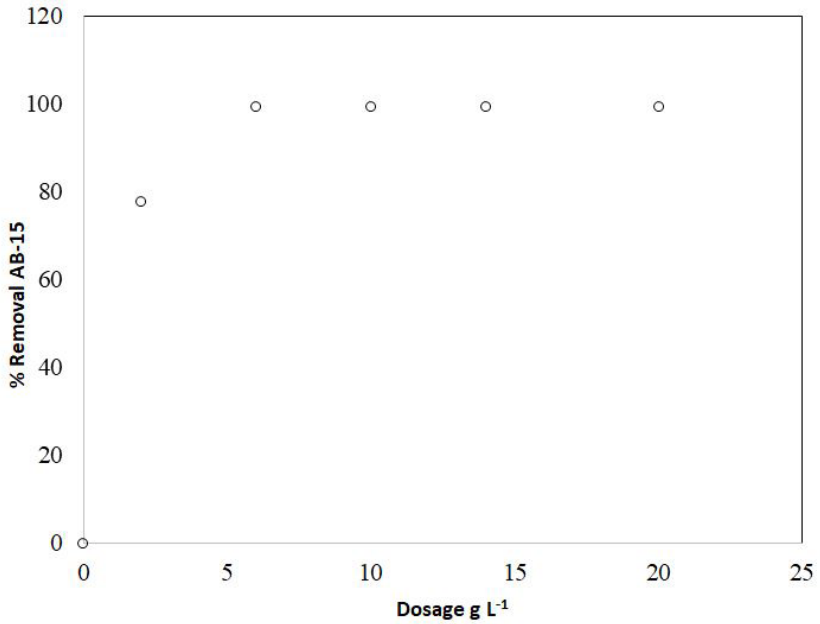

Figure 3: Effect of Fe (III)-chitosan complex sorbent dosage (t = 50 min, 50 ml, T = 35 °C, C_i = 100 mg L^{-1}, 80 rpm, pH_i = 7.00)

The removal percentage of AB-15 from 100 mg L^{-1} solutions using different dosages of Fe (III)-chitosan complex sorbent (2, 6, 10, 14 and 20 g L^{-1}) has been described in Figure 3. The removal percentage increases sharply as the adsorbent dose increases up to dosage = 6 g L^{-1}. This is due to the reason of increasing the number of the iron (III) ion as an active site in the Fe (III)-chitosan sorbent surface area, as mentioned before in pieces of literature [58,60]. The maximum removal (Ca 100%) has been observed using the dosage of 6 g L^{-1}. These results are in line with our study by using chitosan sorbent [54,62], and others such as adsorption of Acid Dyes onto Bentonite and Surfactant-modified Bentonite [60-62].

Effect of pH

Figure 4 represents the removal percentage of AB-15 from 100 mg L^{-1} aqueous solutions using different pH values (2, 4, 7 and 10). The maximum removal percentage Ca 99% is achieved with pH = 10, while it is 88% by using pH = 2. This indicates that a significant influence of the pH value on the sorption process of AB-15 onto Fe (III)-chitosan complex sorbent. In general, the percentage removal of AB-15 from water was higher in basic solutions than in neutral and acidic conditions. From another direction, amino groups (-NH_2) in the Fe (III)-chitosan complex sorbent can be easily protonated to form -NH_3+ groups and eliminate Fe (III) ion from the surface (destroy the Fe (III)-chitosan complex). This lead to decrease the number of the iron ion on the surface and then decrease the active sites and efficiency of sorption AB-15 in the Fe (III)-chitosan complex surface. When the pH increases toward the basic medium (pH > 7), the number of protonated amines decrease. This will fixed the Fe (III) on the surface of chitosan, and the AB-15 interaction increases on the surface. This behavior is confirmed by Borsagli, *et al.* [63].

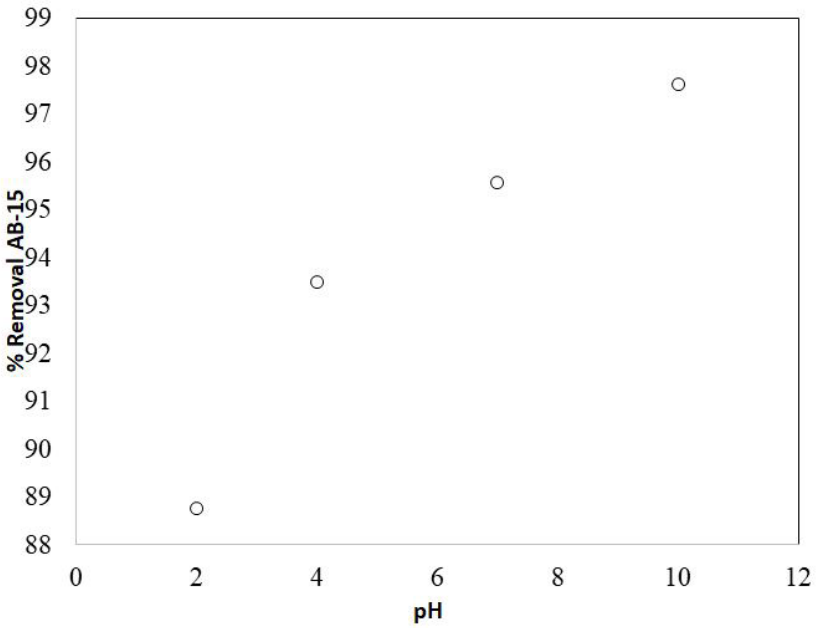

Figure 4: Effect of pH (t = 90 min, C_i= 100 mg L^{-1}, 35 °C, dosage of Fe (III)-chitosan complex = 2 gL^{-1}, 80 rpm)

Adsorption Isotherm

The maximum sorption capacity of AB-15 can be determined by the equilibrium distribution between the Fe (III)-chitosan complex and the solution. For this target, various isotherm models are used to describe the equilibrium such as Langmuir and Freundlich models. Wherein, they are used to fit the experimental and resulted data as reported in selected kinds of literature [57,64-67]. Isotherm studies were conducted at 35 °C by varying the initial concentration of AB-15. The representative initial concentration (10, 30, 50, 70, and 100 mg L^{-1}) of AB-15 were mixed with slurry concentrations (dose) of Fe (III)-chitosan complex (=2 g L^{-1}) for 50 minutes, which was the equilibrium time for the Fe (III)-chitosan complex and AB-15 chemisorptions mixture.

The linear form of the Langmuir model is given by:

$$\frac{C_e}{q_e} = \frac{1}{q_{max} b} + \frac{1}{q_{max}} C_e \qquad (5)$$

Where:

q_e : AB-15 amount (mg) on the Fe (III)-chitosan complex (g) at equilibrium (mg g^{-1}); and q_{max} is the maximum dye uptake per unit dosage of Fe (III)-chitosan complex sorbent (mg g^{-1}), which is related to adsorption capacity. The b is Langmuir constant (L.mg^{-1}) which is exponentially proportional to the heat of adsorption as well as it related to the affinity of binding sites and is a measure of the energy of adsorption. Therefore, a plot of $\frac{C_e}{q_e}$ versus C_e gives a straight line of slope $\frac{1}{q_{max}}$ and intercept $\frac{1}{q_{max} b}$. The thermodynamic and the equilibrium results were obtained at the pH = 7.00 model solution of AB-15, which are summarized in Table 1.

The Langmuir isotherm model is used to fit the experimental data, giving a correlation regression coefficient (R^2= 0.998), which is a measure of goodness-of-fit and the general empirical formula of the Langmuir model by $\frac{C_e}{q_e} = 0.0338C_e + 0.0294$, as shown in Figure 5. Our results are in a good qualitatively agreements with those found from adsorption of AB-15 onto our recent study by using chitosan [54], red muds adsorbent [30] and the adsorption of the Acid Blue-25 (AB-25) onto raw diatomite [68].

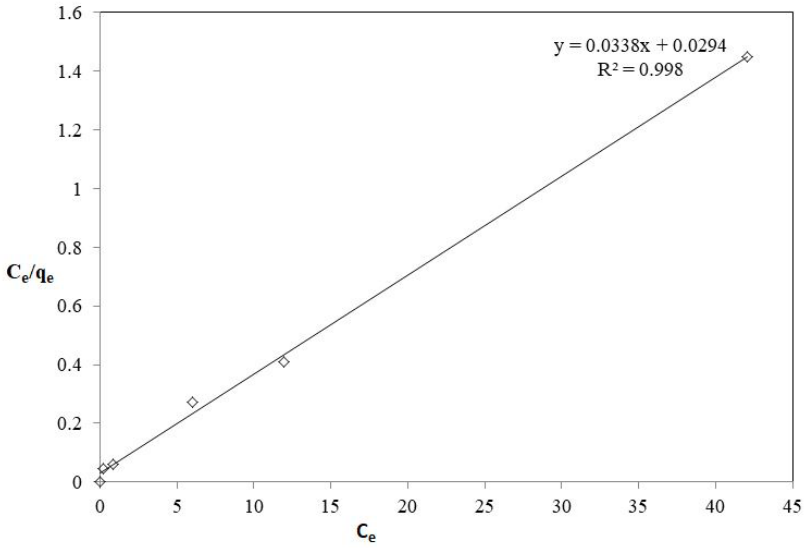

Figure 5: The linearized Langmuir adsorption isotherms for AB-15 adsorption onto Fe (III)-chitosan complex sorbent (dosage = 2 g L^{-1}, Temperature = 35 °C, agitation speed = 80 rpm and contact time = 50 min)

On the other side, the Freundlich model is commonly used to describe the adsorption characteristics of the heterogeneous surface. It represents initial surface adsorption followed by a condensation effect resulting from strong adsorbate-adsorbate interaction.

The linear form of the Freundlich model is also given by:

$$\ln q_e = \ln K_F + \left(\frac{1}{n}\right)\ln C_e \qquad (6)$$

Where K_F and n are Freundlich constants determined from the slope and intercept of plotting ln lnq_e versus $ln\ C_e$.

The experimental data fit into the Freundlich model as shown in Figure 6. The empirical formula of this model is found as $ln\ q_e$=0.9911 $ln\ C_e$ - 1.2619 with R^2= 0.4633. The Langmuir model has a better fitting model than the Freundlich model does. Figure 6 shows that the Langmuir model has a higher correlation regression coefficient (R^2 = 0.998) than the Freundlich model. The smaller the value of the heterogeneity parameter (1/n) means the greater the expected heterogeneity [69,70]. The results exhibit a value of $\frac{1}{n}\left(0 < \left(\frac{1}{n}\right) < 1\right)$ indicating the more heterogeneous physisorptions of AB-15 onto Chitosan as mentioned in the reported works of literature [57,71].

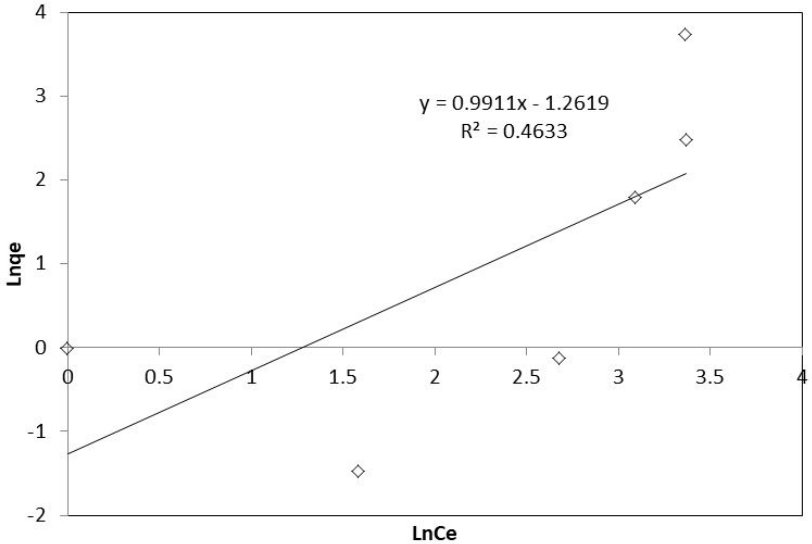

Figure 6: The linearized Freundlich adsorption isotherms for AB-15 adsorption by Fe (III)-chitosan complex sorbent (dosage = 2 g L^{-1}, Temperature = 35 °C, agitation speed = 80 rpm and contact time = 50 min)

The effect of isotherm shape is discussed from the direction of predicting the weather and adsorption system is "favorable or "unfavorable". It was previously reported [71,72] that the dimensional analysis, separation factor, or equilibrium parameters "R_L" was as an essential feature of the Langmuir isotherm to predict adsorption system to be "favorable or "unfavorable" by equation 7:

$$RL = 1/(1+bCi) \quad (7)$$

Where C_i is the initial AB-15 concentration mg L^{-1}. The calculated R_L was less than 1.0, indicating for the favorable adsorption as shown in Figure 7.

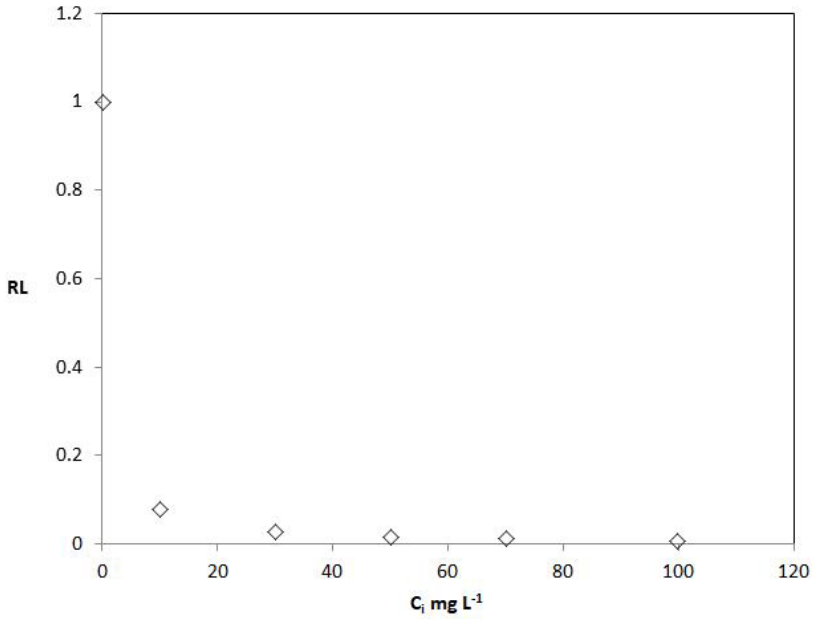

Figure 7: The separation factor of sorption vs. initial concentration of AB-15 dye

The apparent Gibbs free energy of sorption (ΔG^0) is the fundamental criterion of spontaneity. The reaction occurs spontaneously at a given temperature if ΔG^0 is negative in value. The standard Gibbs free energy change (ΔG^0) for the adsorption of AB-15 molecule on the chitosan surface can be calculated using the following thermodynamic equation

$$\Delta G^{\circ} = -RT \ln K_L \quad (8)$$

Wherein, R is the universal gas constant (8.314 J mol^{-1} K^{-1}) and T is the absolute temperature in Kelvin

$$K_L = b \bullet M_A \quad (9)$$

Where M_A is the molar weight of sorbate (AB-15 = 775.95 g mol^{-1}, where K_L =892.110 L mol^{-1}, and b is the equilibrium constant, related to the Langmuir constant, b (=1.1497).

The value of standard Gibbs free energy change calculated at 35 °C is found to be -17.405 kJ mol^{-1}. The negative sign for (ΔG^0) indicates the spontaneous nature of AB-15 adsorption on the Fe (III)-chitosan complex sorbent surface.

To justify the validity of Fe (III)-chitosan complex as a sorbent for the removal of AB-15 from the aqueous solution, the adsorption potentials, as shown in Table 1.

	Adsorbent	Langmuir			Freundlich				
		q_{max} (mg g^{-1})	b (L mg^{-1})	R^2	K_f	—	R^2	Isotherm	Ref
1	Activated carbons prepared from sunflower seed hull	75 - 110		0.994				Langmuir	[43]
2	Mud red	3.11	0.41	0.995	1.74	0.39	0.921	Langmuir	[30]
3	*Azolla filiculoides* biomass	7.11	1.11	0.998	51.2	1.02	0.963	Langmuir	[46]
4	Chitosan	53.76	1.806	0.919	27.5	0.55	0.998	Freundlich	[54]
5	Fe(III)-chitosan complex sorbent	29.586	1.1497	0.998	0.28	0.99	0.463	Langmuir	herein

Table 1: List the compression of the adsorption isotherm of AB-15 onto various adsorbents

Sorption Kinetic Model

Figure 8 shows the effect of contact time regarding the adsorption of Ab-15 onto Fe (III)-chitosan complex sorbent. At the initial stage, the removal rate of AB-15 is high during the first 5 minutes. The initial faster rate may be due to the availability of the uncovered surface area of the Fe (III)-chitosan complex sorbent. The final equilibrium of sorption starts after 40 minutes yielded a maximum removal of 99% (approx.) at T = 55 °C. At the later stages, there is slightly increasing removal efficiency within increasing the contact time. This is due to the decreased or lesser number of iron (III) ion onto Fe (III)-chitosan complex sorbent as an active site. Similar results have been reported in the literature for the removal of dyes by chitosan [54,59] and activated clay [73] adsorbents.

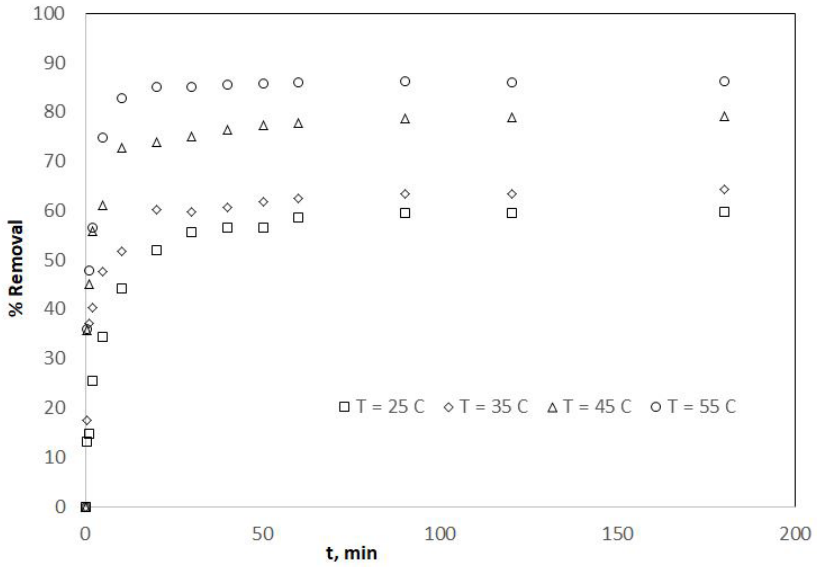

Figure 8: Effect of contact time on AB-15 sorption by using different temperature (25, 35, 45, and 55 °C), dosage = 2 g L^{-1}, 80 rpm, and C_i = 100 mg L^{-1}, pH_i = 7.0

The kinetics sorption models of pseudo-first-order and pseudo-second-order assume that adsorption of AB-15 from the 100 mg L^{-1} of an aqueous solution onto Fe (III)-chitosan complex is a pseudo-chemical reaction. The role of contact time was studied under the shaking conditions, for instance, the pH of the solution was 7.0, 80 rpm, 2 g L^{-1} dosage of Fe (III)-chitosan complex sorbent and by applying 25, 35, 45 or 55 °C. Samples were collected at regular intervals and then analyzed after filtration. The adsorption rate can be determined, respectively, for the pseudo-first-order kinetic model (Eq. 10) [74,75] and the pseudo-second-order kinetic model (Equation 11) [75,76] in their integral expression by the following equations:

$$\ln(q_e - q_t) = \ln q_e - k_1 t \qquad (10)$$

Where q_e and q_t (mg g^{-1}) = the amounts of adsorbed AB-15 at equilibrium and at the time (t), respectively,

k_1 (min^{-1}) = the pseudo-first-order rate constant,
t (minutes) = contact time of adsorption.

The plot of $\ln(q_e - q_t)$ versus t results the determination coefficient value R^2 very small (approx. 0.564). Therefore, the experimental data does not fit to the pseudo-first order. Therefore, it is better to use the pseudo-second-order kinetic model as an integrated form:

$$\frac{t}{q_t} = \frac{1}{k_2 q_e^2} + \frac{t}{q_e} \qquad (11)$$

Where k_2 = the equilibrium rate constant of the pseudo-second-order kinetic model (g mg^{-1} min^{-1}). The plot of $\frac{t}{q_t}$ versus t results the determination coefficient value ca. R^2 = 0.999 as shown in Figure 9. Therefore, the experimental data fit better to the pseudo-second-order. The rate constant of k_2 and q_e can be determined a straight line of slope $1/q_e$ and intercept of $1/(k_2)$ as shown in Table 2.

T, °C	Eq.time (min.)	k_2 (g mg^{-1} min^{-1})	q_e, Exp (mg g^{-1})	q_e, Calc (mg g^{-1})	R^2
25	60	0.01253	29.88913	30.3951	0.9996
35	50	0.02308	39.66522	39.840	0.9999
45	30	0.0192114	32.21957	32.3624	0.9998
55	20	0.04339	43.1413	43.2900	1.0000

Table 2: The parameters of the pseudo-second-order kinetic model

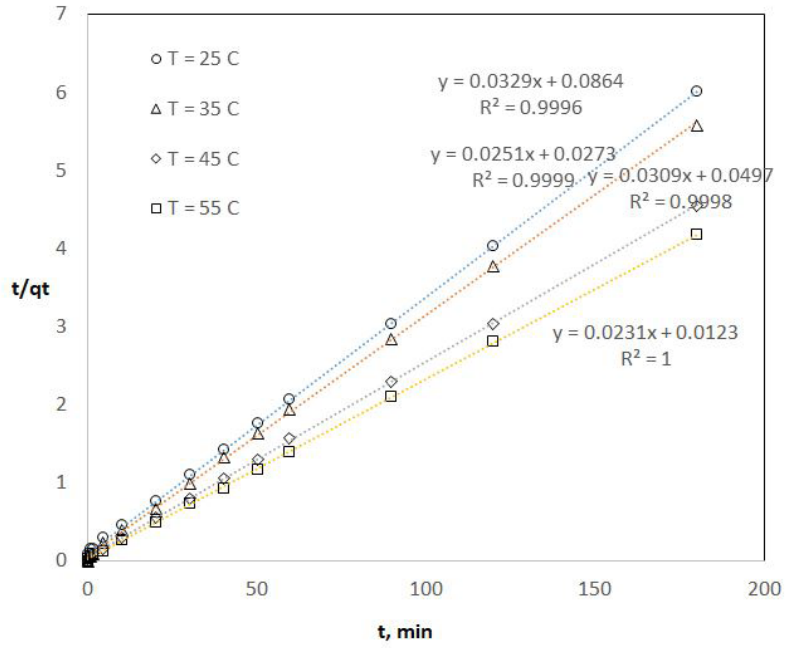

Figure 9: Pseudo-second order model of AB-15 by using different Temperature (25, 35, 45, and 55 °C), dosage = 2 g L^{-1}, 80 rpm, and C_i = 100 mg L^{-1}

The adsorption model of AB-15 transport onto Fe (III)-chitosan complex surfaces are regarded as pseudo-second-order. Furthermore, the compression of q_e values from the experimental work of this study and calculated one of the pseudo-second-order kinetic model (difference smaller) also show the availability of this model (see Figure 10).

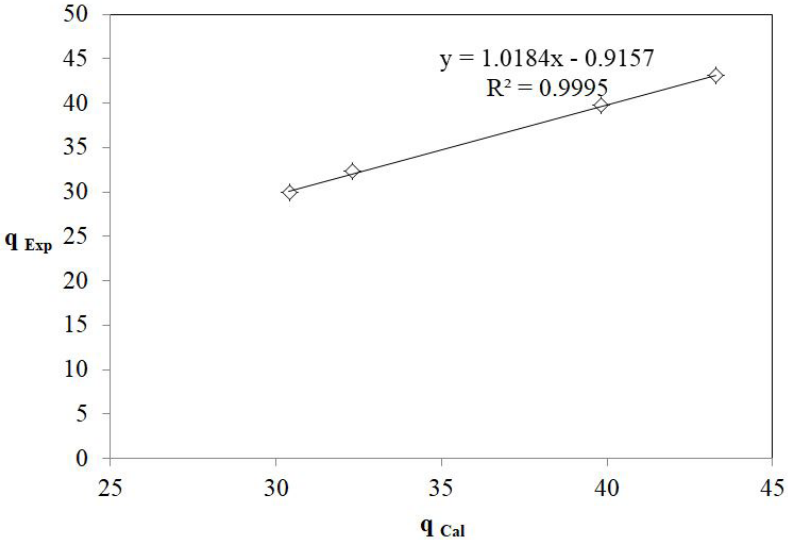

Figure 10: The relationship and trend of the q_{exp}. Vs. q_{cal}. Obtained by Pseudo-second order model

To determine the diffusibility of the AB-15 into the Fe (III)-chitosan complex adsorbent, Weber-Moris intraparticle diffusion model [77] were used in the form of the Equation 12:

$$q_t = k_{int}\sqrt{t} + C \qquad (12)$$

Where C is constant, qt the amount of AB-15 adsorbed at the time (mg g^{-1}) and k_{int} is the intraparticle diffusion rate constant (mg g^{-1} $min^{-0.5}$). A plot of q_t vs. $\sqrt{t}$ giving straight line confirms intraparticle diffusion sorption. Figure 11 shows that the plot is not linear and the moreso do not pass through the origin. The presence of multi-linearity indicates that two or more steps occur, and then the intraparticle diffusion could not be the only mechanism involved. The first, the gradual adsorption stage (from 0 up to 30 minutes of adsorption period) is the external surface adsorption or instantaneous adsorption stage. The second portion is the sharper portion stage (from 30 up to 60 minutes of adsorption period), where the intraparticle diffusion is rate- controlled (k_{int} = 5.8493 mg g^{-1} $min^{-0.5}$ and R^2 = 0.9506, see Figure 11). The third portion is the final equilibrium stage (t > 60 min.) where the intraparticle diffusion starts to slow down due to extremely low solute concentrations in the solution.

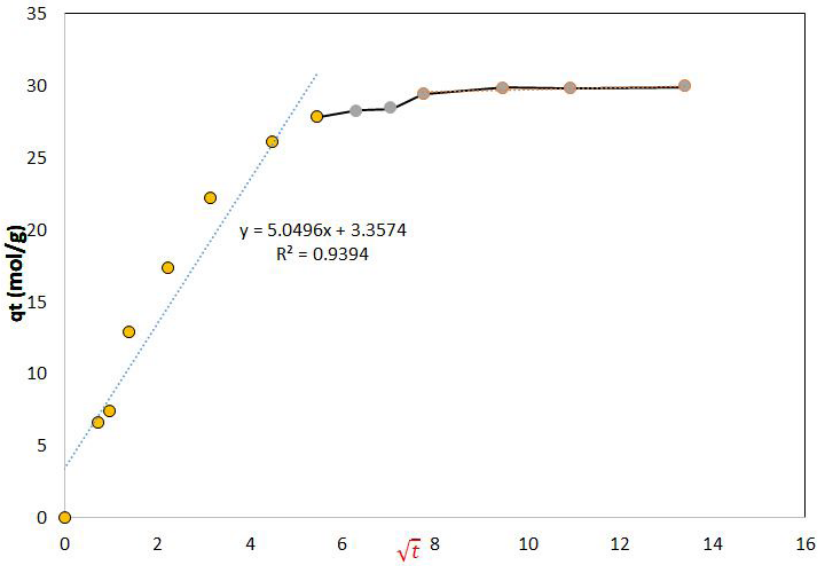

Figure 11: Weber-Moris intra-particular diffusion kinetic model, T = 55 °C, t = 30 min, C_i = 100 mg L^{-1}

Conclusion

In this work, Acid Blue-15 (AB-15) dye is removed from the water using Fe (III)-chitosan complex adsorbent, achieving the highest removal percentage (99%) during the first 50 minutes (equilibrium time) of batch sorption. The sorption of AB-15 by Fe (III)-chitosan complex adsorbent is highly influenced by the initial concentration of AB-15 (C_i = 10 to 100 mg L^{-1}), pH of the basic medium, dosage (> 2 g L^{-1}) and temperature (T = 55 °C).

The sorption of AB-15 onto Chitosan has followed the pseudo-second-order model. The highest kinetic rate constant k_2 of sorption is achieved at T = 55 C. Wherein, the physical meaning indicates that the sorption of AB-15 onto Fe (III)-chitosan complex adsorbent achieve chemisorption. The equilibrium parameter (R_L) is less than 1.0 indicating for the favorable sorption. The experimental isotherm is largely identical with the Langmuir isotherm model. The negative sign for (ΔG^0) indicates the spontaneous nature of AB-15 adsorption on the Fe (III)-chitosan complex adsorbent surface.

Weber-Moris intraparticle diffusion model shows that two or more steps occur as follows: (i) the first stage is the external surface adsorption or instantaneous adsorption stage within 0 up to 30 minutes of adsorption period; (ii) The second stage is the intraparticle diffusion stage (rate- controlled step) within 30 up to 60 minutes of the adsorption period (it is a chemisorption process); (iii) Equilibrium and saturation stage from t>60 min. The final stage is the equilibrium stage where the intraparticle diffusion starts to slow down due to extremely low solute concentrations in the solution

The new information in this study suggests for using the Fe (III)-chitosan complex adsorbent as natural filtering materials for removing the AB-15 from the water.

References

1. Tan Cy, Li G, Lu XQ, Chen Zl (2010) Biosorption of basic orange using dried A. filiculoides. Ecol Engin 36: 1333-40.

2. Garg VK, Renuka G, AnuBala Y, Rakesh K (2003) Dye removal from aqueous solution by adsorption on treated sawdust. Bioresour Technol 89: 121-4.

3. Littlefield NA, Blackwell BN, Hewitt CC, Gaylor DW (1985) Chronic toxicity and carcinogenicity studies of gentian violet in mice. Fundam Appl Toxicol 5: 902-12.

4. Culp SJ, Beland FA (1996) Malachite green: a toxicological review. J Am Coll Toxicol 15: 219-38.

5. Zazouli MA, Balarak D, Mahdavi Y, Ebrahimi M (2013) Adsorption rate of 198 reactive red dyes from aqueous solutions by using activated red mud. Iran J Health Sci 1: 36-43.

6. Venkata Mohan S, Sailaja P, Srimurali M, Karthikeyan, (1999) Color removal of monoazo acid dye from aqueous solution by adsorption and chemical coagulation. Environ Eng Policy 1: 149-54.

7. Wu J, Eiteman MA, Law SE (1998) Evaluation of membrane filtration and ozonation processes for treatment of reactive-dye wastewater. J Environ Eng 124: 272-77.

8. Chun H, Yizhong W (1999) Decolorization and biodegradability of photocatalytic treated azo dyes and wool textile wastewater. Chemosphere 39: 2107-15.

9. Vlyssides AG, Loizidou M, Karlis PK, Zorpas AA, Papaioannou D (1999) Electrochemical oxidation of a textile dye wastewater using a Pt/Ti electrode. J Hazard Mater 70: 41-52.

10. Pearce CL, Lloyd JR, Guthrie JT (2003) The removal of color from textile wastewater using whole bacterial cells: a review. Dyes Pigm 58: 179-96.

11. Sharma DK, Saini HS, Singh M, Chimni SS, Chadha BS (2004) Biodegradation of acid blue-15, a textile dye, by an up-flow immobilized cell bioreactor. J Ind Microbiol Biotechnol 31: 109-14.

12. Seshadri S, Bishop PL, Agha AM (1994) Anaerobic- aerobic treatment of selected azo dyes in wastewater. Waste Manage 15: 127-37.

13. Arami M, Yousefi Limaee N, Mahmoodi NM, Tabrizi NS (2005) Removal of dyes from colored textile wastewater by orange peel adsorbent: Equilibrium and kinetic studies. J Collide interface Sci 288: 371-6.

14. Adeyemo AA, Adeoye IO, Bello OS (2015) Adsorption of dyes using different types of clay: a review. Appl Water Sci 7: 543-68.

15. Kaykhaii M, Sasani M, Marghzari S (2018) Removal of Dyes from the Environment by Adsorption Process. Chem Mat Eng 6: 31-5.

16. Mittal A, Jhare D, Mittal J (2013) Adsorption of hazardous dye eosin yellow from aqueous solution onto waste material De-oiled Soya: isotherm, kinetics and bulk removal. J Mol Liq 179: 133-40.

17. Sivaraj R, Namasivayam C, Kadirvelu K (2001) Orange peel as an adsorbent ın the removal of acid violet 17 (acid dye) from aqueous solutions. Waste Manage 21: 105-10.

18. Walker GM, Hansen L, Hana JA, Allen SJ (2003) Kinetics of a reactive dye adsorption onto dolomitic sorbents. Water Res 37: 2081-9.

19. Özacar M, Şengil A (2003) Adsorption of acid dyes from aqueous solutions by calcined alunite and granular activated carbon. J Hazard Mater 98: 211-24.

20. Ozdemir O, Armagan B, Turan M, Celik MS (2004) Comparison of the adsorption characteristics of azoreactive dyes on mezoporous minerals. Dyes Pigm 62: 49-60.

21. Wang S, Zhu ZH (2005) Sonochemical treatment of fly ash for dye removal from wastewater. J Hazard Mater 126: 91-95.

22. Markandeya, Shukla SP, Dhiman N, Mohan D, Kisku GC, et al. (2017) An Efficient Removal of Disperse Dye from Wastewater Using Zeolite Synthesized from Cenospheres. J Hazard Toxic Radioact Waste 21(4): 04017017.

23. Dotto GL, Moura JM, Cadaval TRS, Pinto LAA (2013) Application of chitosan films for the removal of food dyes from aqueous solutions by adsorption. Chem Eng J 214: 8-16.

24. Toor M, Jin B (2011) Adsorption characteristics, isotherm, kinetics, and diffusion of modified natural bentonite for removing diazo dye. Chem Eng 187: 79-88.

25. Nadaroglu H, Celebi N, Kalkan E, Tozsin G (2013) Water prufication of textile dye acid red 37 adsorption on laccase-modified silica fume. Jökull J 63: 87-113.

26. Zazouli MA, Balarak D, Mahdavi Y, Karimnejad F (2014) Application of Azolla Filiculoides biomass for Acid blue 15 dye (AB15) Removal from aqueous solutions. J Basic Res Med Sc 1: 29-37.

27. Shalaby NH, Ewais EMM, Elsaadany RM, Ahmed A (2017) Rice husk templated water treatment sludge as low cost dye and metal adsorbent. Egypt J Pet 26: 661-8.

28. Balarak D, Jaafari J, Hassani G, Mahdavi Y, Tyagi I, et al. (2015) The use of low-cost adsorbent (Canola residues) for the adsorption of methylene blue from aqueous solution: Isotherm, kinetic and thermodynamic studies. Colloids Interface Sci. Commun 7: 16-19.

29. Balarak D, Pirdadeh F, Mahdavi Y (2015) Biosorption of Acid Red 88 dyes using dried Lemna minor biomass. J Sci Technol Environ Informat 01: 81-90.

30. D Balarak, Y Mahdavi, S Sadeghi (2015) Adsorptive removal of acid blue 15 dye (AB15) from aqueous solutions by red mud: characteristics, isotherm and kinetic studies. Sci J Environ Sci 4: 102-12.

31. Garg V K, Amita M, Kumar R, Gupta R (2004) Basic dye (methylene blue) removal from simulated wastewater by adsorption using Indian Rosewood sawdust: a timber industry waste. Dyes Pigm 63: 243-50.

32. Pavel J, Buchtova H, Ryznarova M (2003) Sorption of dye from aqueous solutions onto fly ash. Water Res 37: 4938-44.

33. Robinson T, Chandran B, Nigam P (2002) Removal of dyes from a synthetic textile dye effluent by biosorption on apple pomace and wheat straw. Water Res 36: 2824-30.

34. Namasivayam C, Muniasamy N, Gayatri K, Rani M, Ranganathan K (1996) Removal of dyes from aqueous solutions by cellulosic waste orange peel. Bioresour Technol 57: 37-43.

35. Arami M, Yousefi Limaee N, Mahmoodi NM, Salman Tabrizi N (2005) Removal of dyes from colored textile wastewater by orange peel adsorbent: equilibrium and kinetic studies. J Colloid Interface Sci 288: 371-6.

36. Doulati Ardejani F, Badii KH, Yousefi Limaee N, Mahmoodi NM, Arami M, et al. (2007) Numerical modelling and laboratory studies on the removal of Direct Red 23 and Direct Red 80 dyes from textile effluents using orange peel, a low-cost adsorbent. Dyes Pigm 73: 178-85.

37. Pishgar M, Yazdanshenas ME, Ghorbani MH, Farizadeh K (2013) Removal of Basic Blue 159 from Aqueous Solution Using Banana Peel as a Low-Cost Adsorbent. J App Chem Res 7: 51-62.

38. Bhattacharyya KG, Sharma A (2003) Adsorption characteristics of the dye, Brilliant Green, on Neem leaf powder. Dyes Pigm 57: 211-22.

39.Tanyildizi MS, Altundogan HS (2017) Removal of Reactive Dye by Using Soybean Cake. Turk J Sci Technol 12: 17-23.

40. Arami M, Limaee NY, Mahmoodi NM (2006) Investigation on the adsorption capability of egg shell membrane towards model textile dyes. Chemosphere 65: 1999-2008.

41. Nethaji S, Sivasamy A (2011) Adsorptive removal of an acid dye by lignocellulosic waste biomass activated carbon: Equilibrium and kinetic studies. Chemosphere 82: 1367-72.

42. Padmesh TVN, Vijayaraghavan K, Sekaran G, Velan M (2006) Biosorption of Acid Blue 15 using fresh water macroalga Azolla filiculoides: Batch and column studies. Dyes Pigm 71: 77-82.

43. Thinakaran N, Baskaralingam P, Ravi KVT, Panneerselvam P, Sivanesan S (2008) Adsorptive Removal of Acid Blue 15: Equilibrium and Kinetic Study. Clean soil Air Water 36: 798-804.

44. Foo K, Hameed B (2011) Preparation and characterization of activated carbon from sunflower seed oil residue via microwave assisted K2CO3 activation. Bioresour Tech 102: 9794-9.

45. Padmesh TVN, Vijayaraghavan K, Sekaran G, Velan M (2006) Application of Azolla rongpong on biosorption of acid red 88, acid green 3, acid orange 7 and acid blue 15 from synthetic solutions. Chem Eng J 122: 55-63.

46. Zazouli MA, Balarak D, Mahdavi Y, Karimnejad F (2014) The application of Azolla filiculoides biomass in acid blue 15 dye (AB15) removal from aqueous solutions. J Bas Res Med Sci 1: 29-37.

47. Sharma D, Saini K, Singh H, Chimni S, Chadha M (2004) Biodegradation of acid blue-15, a textile dye, by an up-flow immobilized cell bioreactor. J Ind Microbiol Biotechnol 31: 109-14.

48. Foo K, Hameed B (2012) Preparation and characterization of activated carbon from melon (Citrullus vulgaris) seed hull by microwave-induced NaOH activation. Desalin Water Treat 47: 130-8.

49. Subramani S, Kumaresan D, Thinakaran N (2015) Application of activated carbon derived from waste Delonix regia seed pods for the adsorption of acid dyes: Kinetic and equilibrium studies. Desalin Water Treat 1-12.

50. Kaur S, Walia TPS, Kaur R (2008) Removal of health hazards causing acidic dyes from aqueous solutions by the process of adsorption. Online J Health Allied Sci 6.

51. Shao Y, Martel B, Morcellet M, Weltrowski M, Crini G (1996) Sorption of textile dyes on β-cyclodextrin-epichlorhydrin gels. J Inclusion Phenom Mol Recognit Chem 25: 209-12.

52. Foo KY, Hameed BH (2011) Microwave assisted preparation of activated carbon from pomelo skin for the removal of anionic and cationic dyes. Chem Eng J 173: 385-90.

53. Devi S, Murugappan A, Rajesh Kannan R (2015) Textile dye wastewater treatment using freshwater algae in packed-bed reactor: Modeling. Desalin Water Treat 57: 17995-8002.

54. Al-Anber MA, Al-Qaisi W (2018) Removal the Acid Blue-15 Dye from Water by Chitosan: Kinetic and Thermodynamic Study. Asian J Green Chem.

55. Burke A, Yilmaz E, Hasirci N, Yilmaz O (2002) Iron (III) Ion Removal from Solution Through Adsorption on Chitosan. J Appl Polymer Sci 84: 1185-92.

56. Al-Anber M (2017) Adsorption Thermodynamics of Inorganic aqueous ferric ion onto rice grain. Biointerface Res Appl Chem 7: 1887-95.

57. Al-Anber M (2011) Thermodynamics Approach in the Adsorption of Heavy Metals, Thermodynamics-Interaction Studies-Solids, Liquids and Gases, Dr. Juan Carlos Moreno-Pirajan (1st Edn) InTech 737-64.

58. Srinivasan A, Viraraghavan T (2010) Decolorization of dye wastewaters by biosorbents: a review. J Environ Manag 91: 1915-29.

59. Sarkar K, Banerjee SL, Kundu PP (2012) Removal of Anionic Dye in Acid Solution by Self Cross-linked Insoluble Dendronized Chitosan. Hydrol Current Res 3:133.

60. Ho YS, Chiang CC, Hsu YC (2011) Sorption Kinetics for Dye Removal from Aqueous Solution Using activated clay. Separation Sci TechnoL 36: 2473-88.

61. Akl MA, Youssef AM, Al-Awadhi MM (2013) Adsorption of Acid Dyes onto Bentonite and Surfactant-modified Bentonite. J Anal Bioanal Tech 4: 174.

62. Yoshida H, Okamoto A, Kataoka T (1993) Adsorption of acid dye on cross-linked Chitosan fibers: equilibria. Chem Eng Sci 48: 2267-72.

63. Medeiros Borsagli FGL, Borsagli A (2019) Chemically Modified Chitosan Bio-Sorbents for the Competitive Complexation of Heavy Metals Ions: A Potential Model for the Treatment of Wastewaters and Industrial Spills. J Polym Environ.

64. Domenico PA, Schwartz FW (1990) Physical and Chemical Hydrogeology (1st Edn) John Wiley and Sons, New York 1-494

65. Reddi LN, Inyang HI (2000) Geo-Environmental Engineering Principles and Applications. CRC Press, Marcel Dekker Inc, New York 492.

66. Nitzsche O, Vereecken H (2002) Modelling Sorption and Exchange Processes in Column Experiments and Large Scale Field Studies. Mine Water Environ 21: 15-23.

67. Zeldowitsch J (1934) On the mechanism of catalytic oxidation of CO and MnO_2 (Über den Mechanismus der katalytischen Oxydation von CO and MnO2). Acta Physicochim URSS 1: 364-449.

68. Badii K, Ardejani FD, Saberi MA, Limaee NY, Shafaei SZ (2010) Adsorption of Acid blue 25 dyes on diatomite in aqueous solutions. Indian J Chemical Technol 17: 7-16.

69. Kinniburgh DG (1986) General-purpose adsorption isotherms. Environ Sci Technol 20: 895-904.

70. Kannan N, Meenakshisundaram M (2002) Adsorption of Congo red on Various Activated Carbons. A Comparative Study. Water Air Soil Poll 138: 289-305.

71. Sejie FP, Nadiye-Tabbiruka MS (2016) Removal of Methyl Orange (MO) from Water by adsorption onto Modified Local Clay (Kaolinite). Phys Chem 6: 39-48.

72. Lagergren S (1898) Zurtheorie of so called adsorption dissolved substances Kungliga. Svenska Vetenskapsakademiens (Zurtheorie der sogenannten adsorption gelösterstoffe Kungliga. Svenska Vetenskapsakademiens) Handlingar 24: 1-39.

73. Siddique BA, Sharma PP, Mohamad S (1999) Adsorption studies on phosphate treated sawdust: Separation of Cr(VI) from Zn(II), Ni(II), Cu(II) and their removal and recovery from electroplating waste. Ind J Environ Prot 19: 846-52.

74. Ho YS, McKay G (1999) Pseudo-second order model for sorption processes. Process Biochem 34: 451-65.

75. Ho YS (2004) Kinetic modeling and equilibrium studies during cadmium biosorption by dead Sargassum sp. biomass by Cruz CCV, da Costa, ACA Henriques CA, Luna AS. Bioresour Technol 93: 321-3.

76. Wong YC, Szeto YS, Cheung WH, McKay G (2004) Pseudo-first-order kinetic studies of the sorption of acid dyes onto Chitosan. Appl polym 92: 1633-45.

77. Weber JWJ, Digiano FA (1996) Process Dynamics in Environmental System; Environmental Science and Technology Series, John Wiley and Sons: New York 943.